

Neutrino oscillations unlocked

Alexei Y Smirnov^{a,b,*}

^a*Max-Planck-Institute für Kernphysik,
Saupfercheckweg 1, Heidelberg, Germany*

^b*International Centre for Theoretical Physics,
Strada Costiera 11, Trieste, Italy*

E-mail: smirnov@mpi-hd.mpg.de

Space-time localization diagrams “unlock” subtle aspects of ν oscillations such as coherence and entanglement. Observability of propagation decoherence in oscillating neutrino state is discussed. The sizes of WPs of reactor and source neutrinos are estimated and it is shown that damping effect due to decoherence is negligible. Among topics of interest are transition from microscopic to macroscopic description of matter effects, oscillations in non-linear generalization of Quantum Mechanics, influence of complex structure of vacuum, in particular, possible presence of cosmic strings and domain walls on oscillations, neutrino oscillations driven by the effective neutrino masses generated via refraction on very light dark matter particles.

*Neutrino Oscillation Workshop-NOW2022
4-11 September, 2022
Rosa Marina (Ostuni, Italy)*

*Speaker

1. Introduction

General idea of this talk was to give an overview of recent advances in the theory of neutrino oscillations as complementary to many experimental talks. The title was suggested by the organizers and I liked it so much that did not asked what “unlocked” means. After my talk Eligio has clarified: that was the first NOW after COVID lock down...

Recent studies (105 papers with neutrino oscillation in titles since September 2021) can be classified using elements of standard neutrino oscillation setup: production, propagation, detection.

At production important issues are creation of coherent states, sizes of the neutrino wave packets, entanglement of neutrinos with accompanying particles.

Propagation: Neutrino oscillations are effect of propagation in space - time. Neutrinos interact with VEV of scalar field(s), $h\langle H \rangle$, which produces masses and mixing. Interesting effects are expected if VEV depend on coordinates: $\langle H \rangle = \langle H(x, t) \rangle$. The coupling can be a function of VEV of some field τ : $h = h(\langle \tau \rangle)$, which in turn depends on coordinates. New studies also include modification of geometry of space-time, metrics, oscillations in the gravitational waves background.

In medium composed of particles and classical fields (e.g. magnetic fields) important aspects of oscillations include (i) transition from microscopic picture (scattering on individual electrons), to macroscopic one in terms of effective potentials; (ii) interactions of neutrinos with scalar bosons (DM particles) and nature of neutrino mass; (iii) oscillations due to refraction: transition from VEV to particle densities $\langle \phi \rangle \rightarrow \phi$; (iv) treatment of oscillating neutrinos in medium as open system, *etc.*

At detection features of interference and coherence were explored.

Oscillations are the quantum mechanical effect (based on superposition and interference): Therefore important issues are tests of QM and quantumness with neutrinos, modification of QM and therefore, evolution equation, *etc.*

This talk covers few aspects mentioned above: (i) space-time localization diagrams; (ii) coherence, entanglement and wave packets; (iii) matter and vacuum effects on propagation.

2. Space-time localization diagrams

The diagrams (Fig. 1) reflect computations of oscillation probabilities in QFT, and visualize various subtle issues unlocking the underlying physics [1]. For simplicity we use the 2ν framework.

The produced and then propagated neutrino state can be presented as

$$|\nu^P\rangle = \psi_1^P(x - v_1 t)|\nu_1\rangle + \psi_2^P(x - v_2 t)|\nu_2\rangle, \quad (1)$$

where ψ_i^P are the wave packets, and v_i are group velocities of mass eigenstates. (The production region is around $x, t = 0$). The detected state is

$$|\nu^D\rangle = \psi_1^D(x - x_D, t - t_D)|\nu_1\rangle + \psi_2^D(x - x_D, t - t_D)|\nu_2\rangle, \quad (2)$$

here ψ_i^D are the detection WP with (x_D, t_D) being the coordinates of center of detection region. Amplitude of oscillations is given by projection of the propagated state onto the detection state: $A(x_D, t_D) = \langle \nu^D | \nu^P \rangle$. For simplicity one can take

$$\psi_i^D(x - x_D, t - t_D) = \delta(x - L)\psi_i^D(t - t_D), \quad (3)$$

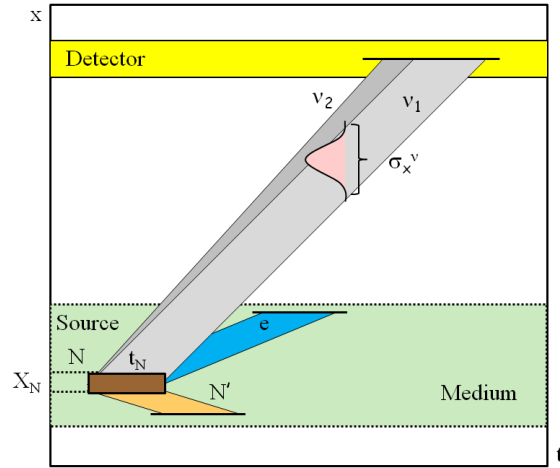


Figure 1: Space-time localization diagram for oscillations of neutrinos produced in beta decay. Shown are $x - t$ localization areas of the decaying nucleus (brown), daughter nucleus (orange), electron (blue) and neutrino mass states (gray). The slopes are determined by group velocities of particles. Yellow rectangle shows localization of the detection process (see details latter).

where L is the baseline. Then after integration over x one obtains

$$A(L, t_D) = \sum_i A_i(L, t_D) = \sum_i \int dt \psi_i^{D*}(t - t_D) \psi_i^P(L - v_i t). \quad (4)$$

Here $A_i(L, t_D)$ can be treated as the generalized WP which includes localizations of both production and detection processes. The oscillation probability equals

$$P(L) = \int dt_D |A(L, t_D)|^2 = \int dt_D [|A_1(L, t_D)|^2 + |A_2(L, t_D)|^2] \quad (5)$$

$$+ 2\text{Re} \int dt_D A_1(L, t_D)^* A_2(L, t_D). \quad (6)$$

Further integration should be done over interval of baseline L due to finite sizes of the source and detector. In what follows we will consider production and detection separately and refer to WP as the produced and propagating WP. The spread of individual WP in the course of propagation is neglected.

At the detection there are two extreme cases determined by time widths of the produced, σ_t^P , and detected, σ_t^D , WPs.

1. Short coherence time of detection $\sigma_t^D \ll \sigma_t^P$. In this case $\psi_i^D(t - t_D) \propto \delta(t - t_D)$, and consequently, according to Eq. (4)

$$A_i(L, t_D) = \psi_i^P(L - v_i t_D). \quad (7)$$

Therefore the interference (6) is determined by overlap of the produced WPs (Fig. 2, left).

2. Long coherence time of detection $\sigma_t^D \gg \sigma_t^P$. In this case

$$A_i(L, t_D) \sim \psi_i^D(L/v_i - t_D). \quad (8)$$

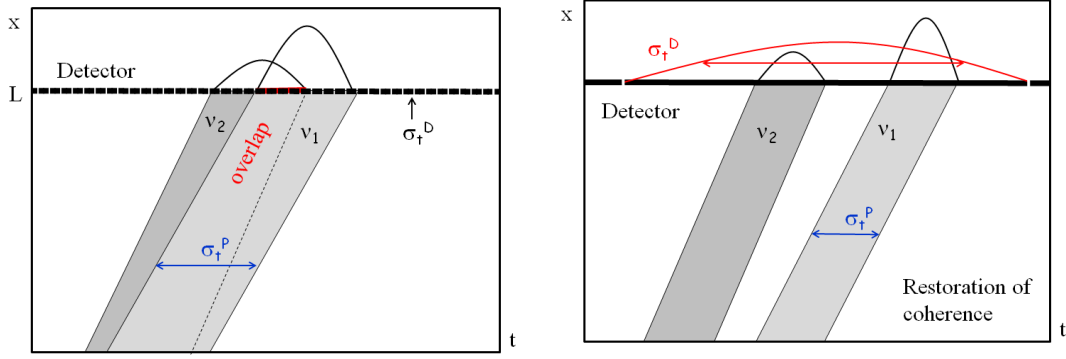


Figure 2: The $x - t$ localization of the detection process. Black narrow rectangles show coherent areas of detection; grey bands show localizations of neutrino mass eigenstates. Left: short coherence time of detection: interference and oscillations are determined by overlap of the WP neutrino bands. Right: long coherence time of detection - restoration of coherence in spite of separation of WPs.

The WP are separated when t_{sep} - the time interval between arrived WP is bigger than σ_t^P . If however $\sigma_t^D \gg t_{sep}$, restoration of coherence occurs (see Fig. 2, right). In other terms the detection process enlarges the arriving WPs so that they start to overlap.

Production: WP's are determined by localization region of the production process: by overlap of localization regions of all particles involved but neutrinos. Consider, e.g. the β -decay: $N \rightarrow N' + e^- + \bar{\nu}$. If N' and e^- are not detected or their interactions can be neglected, localization of the process is given by localization of the parent nucleus X_N . The latter is determined by time between two collisions of atom contained nucleus N , t_N . Then spatial size of the neutrino WP equals

$$\sigma_x \simeq v_\nu t_N \simeq X_N \frac{v_\nu}{v_N} \approx X_N \frac{c}{v_N}.$$

Here c/v_N is huge enhancement factor, so that $\sigma_x \gg X_N$ (Fig. 3, left). In addition, one should take into account entanglement between neutrinos and particles produced together with neutrinos. If N' or/and e^- are detected or interact, this may narrow the interval t_N , and therefore the neutrino WP (Fig. 3, right). If e^- is detected during time interval $t_e < t_N$, the size of ν WP will be determined by t_e . If e^- interacts with particles of medium which have very short time between collisions, t_{coll} , then $\sigma_x \simeq ct_{coll}$. This entanglement is similar to the entanglement in the EPR paradox. To understand this one can consider ν emission and interactions of e^- as a unique process $N A \rightarrow \bar{\nu} e^- N' A$. Contributions to its amplitude from different $x - t$ interactions regions of e^- appear with random phases ξ_k : $A_{tot} = \sum_k A_k e^{i\xi_k}$ (Fig. 3, right), and therefore in the probability they will sum up incoherently.

3. Coherence, entanglement and wave packets

In $x - t$ space separation of wave packets of mass states occurs due to difference of group velocities. This is equivalent to integration over the energy uncertainty. Suppression of interference leads to damping of oscillations: Survival probability can be written as

$$P_{ee} = \bar{P}_{ee} + 0.5D(E, L) \sin^2 \theta \cos \phi, \quad (9)$$

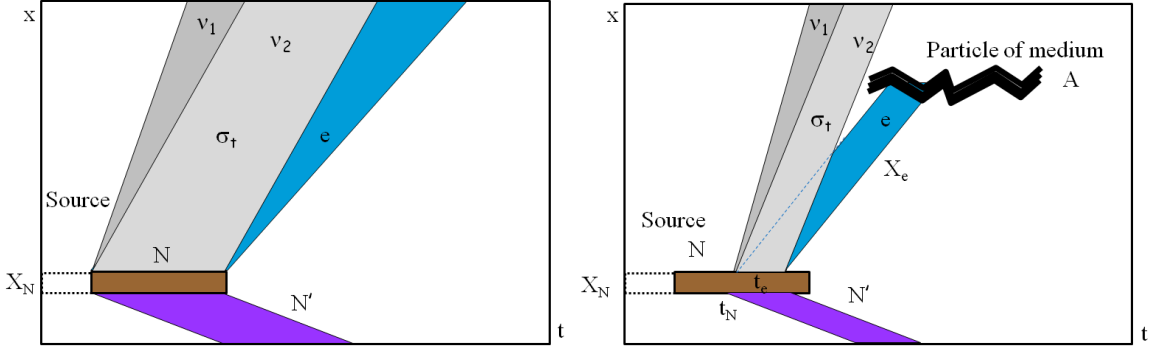


Figure 3: The $x - t$ localization of the production process. Left: accompanying particles (recoil and electron) are not detected or their interactions are negligible. Right: electron interacts with particle of medium A and A has short mean free path (shorter than t_N). This localizes better the electron and therefore neutrino mass states. As a result, the overlap becomes smaller and interference is suppressed.

where the damping factor $D(E, L)$ for Gaussian WP equals

$$D(E, L) = \exp[-0.5(L/L_{coh})^2].$$

Here L_{coh} is the coherence length

$$L_{coh} = \sigma_x \frac{2E^2}{\Delta m^2}.$$

Recall that separation of WP leads to the *propagation decoherence*, in contrast to irreversible QM decoherence. In the former case the information is not lost and can be restored at detection.

The smaller E , the smaller L_{coh} , therefore reactor neutrinos and neutrinos from nuclear sources are most suitable to search for decoherence effects. The absence of damping means that $L \ll L_{coh}$ or explicitly

$$\sigma_x \gg L \frac{\Delta m^2}{2E^2} \quad (10)$$

giving the lower bound on σ_x . Analysis of Daya Bay, RENO and KamLAND data leads to [2]:

$$\sigma_x > 2.1 \cdot 10^{-11} \text{ cm (90\% C.L.)}. \quad (11)$$

Actually, this bound corresponds to the energy resolution of the detectors δ_E : $\sigma_x \sim 1/\delta_E$. Absence of the damping due to finite momentum spread σ_p in Daya Bay allows to put the upper bound [3] $\sigma_p/p < 0.23$ (95% C.L.) at $p = 3$ MeV, which corresponds to $\sigma_x > 1/\sigma_E = 2.8 \cdot 10^{-11}$ cm, similar to that in (11). In future JUNO can improve the limit down to $\sigma_p/p < 0.01$ (95% C.L.) or $\sigma_x > 2.3 \cdot 10^{-10}$ cm [4].

Damping effects in the active - sterile neutrino oscillations were computed for various experiments [5]. Taking for all experiments the same value σ_x (11) found in [2] as the bound, the authors arrived at the following conclusions: (i) decoherence allows to reconcile BEST result with reactor bounds; (ii) results of analysis of experimental data should be presented in two forms: with and without decoherence. In [6] it was argued that these conclusion are based on incorrect value of σ_x .

Propagation decoherence and energy resolution: Integration over the energy resolution of experimental setup described by $R(E_r, E)$ with width δ_E is another sources of damping. It includes

the energy spectrum of produced neutrinos, or/and energy resolution of a detector. The WP of produced neutrino in the energy representation, $f(E, \bar{E})$, acts on oscillations, as R does, and can be attached to $R(E_r, E)$ [6]. In this case the effective resolution function can be introduced:

$$R_{\text{eff}}(E_r, E) = \int d\bar{E} R(E_r, \bar{E}) |f(E, \bar{E})|^2.$$

For Gaussian f and R , R_{eff} is also Gaussian with width $\delta_E^2 + \sigma_E^2$. The problem is to disentangle the two contributions.

For reactor neutrinos the source is β -decays $N \rightarrow N' + e^- + \bar{\nu}$ of fragments of nuclear fission $N N'$ quickly thermalizes and in the moment of decay turns out to be in equilibrium with medium with temperature T . Therefore the average velocity: $v_N \sim [3T/m_N]^{-1/2}$. If N' and e^- interactions can be neglected, localization of ν production process is given by localization of N :

$$\sigma_x \approx v_N t_N \approx X_N c / v_N,$$

where t_N is the time between two essential (with momentum transfer $\Delta p \geq 1/\sigma_x$) collisions of atom containing N with other atoms:

$$t_N \approx [\sigma_{AA} n_U v_N]^{-1}.$$

Here σ_{AA} is the geometric cross-section $\sigma_{AA} \approx \pi(2r_{vdW})^2$, where r_{vdW} is the Van der Waals radius, n_U is the number density of Uranium. Then

$$\sigma_x \approx 2.8 \cdot 10^{-3} \text{ cm.} \quad (12)$$

Effect of accompanying neutrino particles: Its “short cut” estimation can be done taking that duration of ν production process equals the shortest mean free time among mean free times of particles involved [6]. It was shown in [6] that electrons have the shortest time $\sigma_t = t_e = X_e / v_e$, where X_e is determined by ionization of uranium atom by e , σ_{eU} : $X_e = (n_U \sigma_{eU})^{-1}$. This gives

$$\sigma_x = 2 \cdot 10^{-5} \text{ cm,} \quad (13)$$

which can be considered as the upper bound on σ_x .

Another approach is to follow interactions of accompanying particles which determine their $x-t$ localizations. Considering a chain of secondary processes like $e + A \rightarrow e' + A'$ till thermalization of e^- gives $\sigma_x = (5 - 10) \times 10^{-5} \text{ cm}$.

Thus, $\sigma_x / \sigma_x^{exp} \approx 10^5 \div 10^6$, that is, $\sigma_x \gg \sigma_x^{exp}$ where σ_x^{exp} is given in (11). The corresponding energy uncertainty is $\sigma_E \sim 1 \text{ eV}$, while energy resolution $\delta_E \sim 10^5 \text{ eV}$. Therefore to be sensitive to WP's separation the energy resolution function should be known with better than 10^{-5} accuracy. For the Cr -source $\sigma_x = 1.4 \cdot 10^{-5} \text{ cm}$ is obtained [6]. Thus, if additional damping is found, it is due to some new physics and not due to WP's separation.

Large Δm^2 does not help to enhance the decoherence since oscillatory pattern shows up at $L \sim l_\nu$. But $L_{coh} \sim l_\nu \sim 1/\Delta m^2$ and therefore Δm^2 cancels in damping factor which depends on $L/L_{coh} \approx l_\nu/L_{osc}$. Do situations exist in which effect of separation of WP can be tested? Among directions to think are experiments with $L \sim L_{coh}$, lower energies, artificial widening of lines, e.g. by laser irradiation.

In [7] validity of estimations of sizes of WP (12, 13), and consequently, non-unobservability of WP separation were questioned and reply was published in [8]. In particular, it was claimed in [7] that nuclear interactions inside nucleus measure position of parent particle (nucleon), and thus give much smaller sizes of the neutrino WPs, $\sigma_x \sim 1/r_{\text{nucleus}}$, than in (12, 13). According to [6] WP lengths are determined by the absolute localization of parent particle in the oscillation setup, *i.e.*, by the largest spatial uncertainty. The latter is given by localization of atom with decaying nucleus with respect to other atoms in the source. Notice that for reactor neutrinos de Broglie wave is much larger than the size of nucleus, and therefore neutrino is not sensitive to nuclear structure.

4. Matter, vacuum and propagation

From micro to macro picture. Three different approaches were elaborated: (i) a coarse graining and space coordinate averaging over macroscopic volumes with large number of point-like scatterers [9], (ii) summation of potentials produced by individual scatterers on the way of neutrino [10]; (iii) taking into account uncertainty in localization of scatterers X_e . For the weak interactions r_{WI} , usually $X_e \gg r_{\text{WI}}$, where e.g. X_e is localization of e in atom [11].

Since $\lambda_\nu \sim 1/p_\nu \ll X_e$ it makes sense to consider propagation of neutrino inside individual atom with density profile given by wave functions of electrons. Modeling of medium with individual scatterers can be done using the castle wall profile: alternating layers of matter with lengths L_a, L_b and potentials V_a, V_b . This determines mixing angles θ_a, θ_b and half – phases: ϕ_a, ϕ_b acquired in the layers. Oscillation probability is given by [12]

$$P = [1 - I_2/(1 - R_2)] \sin 2(n\zeta),$$

where $\zeta = \arccos R$, n -number of periods, and I, R are known functions of $\phi_a, \phi_b, \theta_a, \theta_b$. For $\phi_a, \phi_b \ll 1$ the probability can be reduced to

$$P = \sin^2 2\theta_m(\bar{V}) \sin^2 0.5\phi(\bar{V}),$$

where

$$\bar{V} \equiv \frac{V_a L_a + V_b L_b}{L_a + L_b}$$

is nothing but the average potential, as is expected in the standard picture.

WP's and non-adiabatic evolution: Partially ionized (or non ionized) atoms can be considered as the electron density perturbations. Number density profile of electrons in atom (O, C, He) is non adiabatic [13]. The interplay of non-adiabatic evolution and separation (relative shift) of the WP's leads to new effects: additional averaging of oscillations [13] with applications to supernova neutrinos. No new effects is expected without WP separation and in the case of adiabatic evolution [13]. Also no new effects appear for a profile with very sharp (step-like) density changes (as in castle wall case).

However, one can show that no new effects are realized also in the case of non-adiabatic evolution of WP's. Indeed, WP's are formed at the production (at boundaries):

$$\psi(t, x) = \int dp f(p) \phi_p(t, x),$$

where $\phi_p(t, x)$ are the plane waves. If there is no absorption or p -dependent interactions, $f(p)$ does not change in the process of evolution. Inserting ψ in the evolution equation $id\psi/dt - H\psi = 0$ and permuting integration over p and evolution we find

$$\int dp f(p) [id\phi_p/dt - H\phi_p] = 0.$$

Superposition principle and linearity of the evolution equation allow to solve first, equation for ϕ_p , and then integrate over p (form the WPs). No new effects predicted in [13] are realized. In the $t - x$ space WP can change form in the course of evolution, but result integrated over time coincides with result in the $E - p$ representation [14]. The conclusion is not clear in the case of $\nu\nu$ -scattering when the Hamiltonian $H = H(\phi_p)$ leads to non-linear evolution equation.

Non-linear generalization of QM. Neutrino oscillations are the QM phenomenon, and therefore modifications of QM affect oscillations and inversely, oscillations can be used to search for deviations from canonical QM. In [15] Schrodinger equation for single particle (with Hamiltonian H_0) was modified as

$$idv(t, x)/dt = \left[H_0 + \epsilon \frac{q^2}{4\pi} \int d^4x' |\nu(t', x')|^2 G_r(t, x; t', x') \right] \nu(t, x). \quad (14)$$

Here G_r is the retarded Green function for scalar (Higgs) field ϕ , q is charge - Yukawa coupling constant of ν and ϕ : $q = m_\nu/\nu$. In this framework the produced neutrino state $\nu^{(p)}$ evolves as [16]

$$\nu^{(p)}(t) = U[t, t_p, \nu^{(p)}] \nu^{(p)}(t_p), \quad (15)$$

where the evolution operator U depends on $\nu^{(p)}$ via integral in (14) thus making the problem non-linear. The operator can be parametrized as

$$U(t, t_p, \nu^{(p)}(t)) = U_0(t, t_p) + \epsilon U_1[t, t_p, \nu^{(p)}].$$

Here the first term is the standard linear evolution matrix, while the second one is the first non-linear correction with ϵ being the expansion parameter. Consequently, the evolving state (15) can be written as

$$\nu^{(p)}(t) = \nu^{(p,0)}(t) + \epsilon \nu^{(p,1)}(t).$$

Equation for the correction $\nu^{(p,1)}(t)$ in coordinate representation is

$$id\nu^{(p,1)}(t)/dt = H_0\nu^{(p,1)}(t) + G[t, x, \nu^{(p,0)}]$$

with the last inhomogeneous term. In [16] to construct G the Yukawa interactions of neutrinos with scalar field ($\nu\nu\phi$) used which originate from the D5 Weinberg's operator. Eventually the oscillation transition probability was computed:

$$P = \sin^2 2\theta \left[\sin^2 \frac{1}{2}\phi - \frac{\epsilon'}{4} \frac{m_1 - m_2}{m_1 + m_2} \sin \phi \right],$$

where the correction $\epsilon' \equiv 81.5\epsilon(m_1 + m_2)^2/\nu^2$ is very small.

Vacuum and properties of oscillations. It was proposed [17] that neutrino vacuum condensate exists due to gravity. The order parameter is fixed by the observed values of neutrino mass

$$\langle \Phi_{\alpha\beta} \rangle = \langle \nu_\alpha^T C \nu_\beta \rangle \simeq \Lambda_G = \text{meV} - 0.1 \text{ eV}.$$

Here ν_α, ν_β are flavor neutrino states fixed by weak (CC) interactions and charged leptons with mass generated by usual Higgs field. The condensate leads to cosmological phase transition at $T \sim \Lambda_G$ at which neutrinos get masses $m_{\alpha\beta} \simeq \langle \Phi_{\alpha\beta} \rangle$, and the mass matrix can be written as $m = U(\theta)^T \langle \Phi \rangle U(\theta)$, where $\langle \Phi \rangle \equiv \text{diag}(\Phi_{11}, \Phi_{22}, \Phi_{33})$, and $U(\theta)$ is the mixing matrix. At $T < \Lambda_G$ the relic neutrinos form bound states $\phi = \nu_\alpha^T C \nu_\beta$, they decay and annihilate into ϕ forming “neutrinoless” Universe. The flavor symmetry of system, $SU(3) \times U(1)$, is spontaneously broken by the neutrino condensate with ϕ being the Goldstone bosons. ϕ get small masses due to explicit symmetry breaking by weak interactions via loops.

Symmetry breaking: $SU(3) \rightarrow Z_2 \times Z_2 \rightarrow I$ produces global topological strings in the first step and domain walls in the second one, thus forming the string-wall network [18]. The length scale of strings and inter-string separation equal

$$\xi \simeq 10^{14} \text{ m} (\lambda/a_G) (\Lambda_G/1\text{meV})^{7/2}, \quad (16)$$

where λ is self-coupling of string field Φ , and a_G is the scale factor of phase transition.

Travelling around string winds VEV $\langle \Phi \rangle$ by the $SU(3)$ transformation:

$$\langle \Phi(\theta_s) \rangle = \omega(\theta_s)^T \langle \Phi \rangle \omega(\theta_s), \quad (17)$$

where $\omega(\theta_s)$ is the path transformation with angles $\theta_s = (\theta_s^{12}, \theta_s^{13}, \theta_s^{23})$. After the path ω the lepton mixing changes as $U = U(\theta)\omega(\theta_s)$ and over length ξ , $\theta_s = O(1)$. The effect is observable: e.g. the solar system moves through the frozen string-wall background with $v = 230 \text{ km/sec}$. For 6 years of Daya Bay operation the distance traveled is $d = vt = 4 \cdot 10^{13} \text{ m}$, which is comparable to the expected ξ (16).

VEV or refraction on scalar DM? Elastic forward scattering of ν on background scalars ϕ (DM) with fermionic mediator χ produces effective potential [19]. It has resonance at $s = m_\chi^2$. For ϕ at rest the resonance ν energy equals

$$E_R = \frac{m_\chi^2}{2m_\phi}.$$

For small m_ϕ the resonance is at low observable energies [20]. At $E \ll E_R$ the potential converges to the Wolfenstein limit. At high energies $E \gg E_R$ it has $1/E$ tail.

In the Hamiltonian of propagation the contribution of potential can be written similarly to the standard vacuum term as $\Delta m_{\text{eff}}^2/2E$. Here

$$\Delta m_{\text{eff}}^2 = 2EV$$

has the following limits (Fig. 4)

$$\Delta m_{\text{eff}}^2 \approx \frac{y^2 n_\phi}{4m_\phi} \begin{cases} 1, & E \gg E_R \\ \epsilon \frac{E}{E_R}, & E \ll E_R \end{cases},$$

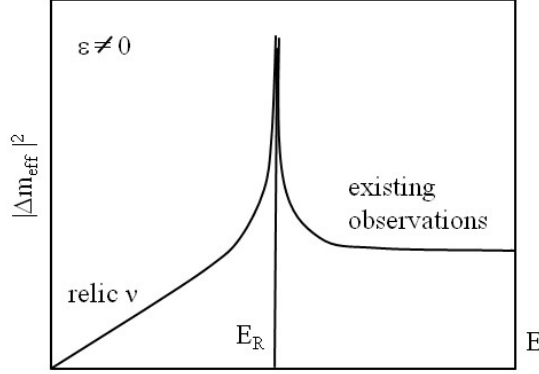


Figure 4: Dependence of the effective (refractive) neutrino mass squared on neutrino energy.

where ϵ is the C-asymmetry of background, y is coupling constant of neutrino and ϕ , n_ϕ is the number density of ϕ . At high energies $\Delta m_{\text{eff}}^2 = \text{const}$ and it has the same features as the vacuum Δm^2 . Therefore in principle oscillations can be explained by Δm_{eff}^2 , if E_R is much below the energies at which neutrino oscillations were observed, that is, much below 0.1 MeV (solar neutrinos).

On the other hand below the resonance (Fig. 4) Δm_{eff}^2 decreases with energy. For $E_R = 0.01$ MeV (and $\epsilon = 1$) we find that in KATRIN experiment with $E \simeq 1$ eV the effective mass $m_{\text{eff}} \equiv \sqrt{\Delta m_{\text{eff}}^2} < 5 \cdot 10^{-4}$ eV, *i.e.* undetectable. The decrease of m_{eff}^2 with energy allows one to avoid the cosmological bound on sum of neutrino masses. Indeed, $m_{\text{eff}}^2 \propto \bar{n}_\phi \propto (1+z)^3$, where \bar{n}_ϕ is the average density of ϕ in the Universe. That is, Δm_{eff}^2 increased in the past, while VEV is constant. For relic ν at $z = 0$: $E \simeq 10^{-4}$ eV, and therefore for the average density of DM in the Universe (the local overdensity 10^5) we have $m_{\text{eff}}^2(0) < 2.5 \cdot 10^{-16}$ eV². At the epoch of matter-radiation equality (when structures in the Universe started to grow) we obtain $m_{\text{eff}}^2(1000) \simeq 2.5 \cdot 10^{-7}$ eV² and $m_{\text{eff}}(1000) \simeq 5 \cdot 10^{-4}$ eV, which satisfies the cosmological bound. Even much smaller masses are obtained in the case of $\epsilon = 0$, when m_{eff}^2 decreases as y^2 [21]. Existing astrophysical and laboratory bounds are satisfied, e.g., for $m_\chi \leq 10^{-3}$ eV, $m_\phi \leq 10^{-10}$ eV, $y \leq 10^{-10}$ [22].

5. Conclusion

Space-time localization diagrams allow to "unlock" the key aspects of neutrino oscillations. Neutrino oscillations are the tool for explorations of properties of space and time, subtle aspects of QM, fundamental symmetries (beyond measurements of neutrino parameters). Effect of propagation decoherence (damping) is unobservable in the present reactor and source experiments. If some additional damping is found, this will be due to new physics.

Evolution of ν state and formation of WP in the momentum space commute, so that propagation decoherence is boundary (in linear case) phenomenon.

Effects of complex structure of vacuum, neutrino condensates, non-linear generalizations of QM affect neutrino oscillations. Studies of neutrino oscillations allow to search for these effects. In this connection searches for time, space and energy dependencies of oscillation parameters is crucial.

Acknowledgements

The author is thankful to Evgeny Akhmedov for numerous discussions.

References

- [1] E. Akhmedov, D. Hernandez and A. Smirnov, *JHEP* **04** (2012), 052 [arXiv:1201.4128 [hep-ph]].
- [2] A. de Gouvêa, V. De Romeri and C. A. Ternes, *JHEP* **06** (2021), 042 [arXiv:2104.05806 [hep-ph]].
- [3] F. P. An *et al.* [Daya Bay], *Eur. Phys. J. C* **77** (2017) no.9, 606 [arXiv:1608.01661 [hep-ex]].
- [4] J. Wang *et al.* [JUNO], *JHEP* **06** (2022), 062 [arXiv:2112.14450 [hep-ex]].
- [5] C. A. Argüelles, T. Bertólez-Martínez and J. Salvado, [arXiv:2201.05108 [hep-ph]].
- [6] E. Akhmedov and A. Y. Smirnov, *JHEP* **11** (2022), 082 [arXiv:2208.03736 [hep-ph]].
- [7] B. J. P. Jones, [arXiv:2209.00561 [hep-ph]].
- [8] E. Akhmedov and A. Y. Smirnov, [arXiv:2210.01547 [hep-ph]].
- [9] E. Akhmedov, *JHEP* **02** (2021), 107 [arXiv:2010.07847 [hep-ph]].
- [10] A. Y. Smirnov and X. J. Xu, *JHEP* **12** (2019), 046 [arXiv:1909.07505 [hep-ph]].
- [11] G. Fantini, A. Gallo Rosso, F. Vissani and V. Zema, *Adv. Ser. Direct. High Energy Phys.* **28** (2018), 37-119 [arXiv:1802.05781 [hep-ph]].
- [12] E. K. Akhmedov, *Nucl. Phys. B* **538** (1999), 25-51 [arXiv:hep-ph/9805272 [hep-ph]].
- [13] M. Kusakabe, [arXiv:2109.11942 [hep-ph]].
- [14] Y. P. Porto-Silva and A. Y. Smirnov, *JCAP* **06** (2021), 029 [arXiv:2103.10149 [hep-ph]].
- [15] D. E. Kaplan and S. Rajendran, *Phys. Rev. D* **105** (2022) no.5, 055002 [arXiv:2106.10576].
- [16] T. Gherghetta and A. Shkerin, [arXiv:2208.10567 [hep-th]].
- [17] G. Dvali and L. Funcke, *Phys. Rev. D* **93** (2016) no.11, 113002 [arXiv:1602.03191 [hep-ph]].
- [18] G. Dvali, L. Funcke and T. Vachaspati, [arXiv:2112.02107 [hep-ph]].
- [19] S. F. Ge and H. Murayama, [arXiv:1904.02518 [hep-ph]].
K. Y. Choi, E. J. Chun and J. Kim, *Phys. Dark Univ.* **30** (2020), 100606 [arXiv:1909.10478].
- [20] A. Y. Smirnov and V. B. Valera, *JHEP* **09** (2021), 177 [arXiv:2106.13829 [hep-ph]].
- [21] M. Sen and A. Y. Smirnov, in preparation.
- [22] K. Y. Choi, E. J. Chun and J. Kim, [arXiv:2012.09474 [hep-ph]].